

Measurement Notes

Note 15

CLEARED
FOR PUBLIC RELEASE
AFRLIDE-PA
28 JUN 01

THE EFFECT OF BANDWIDTH ON ZERO CROSSING

May 1, 1973

J. E. Faulkner
NDRC, Inc.
Suite 804, 5301 Central N. E.
Albuquerque, New Mexico 87108

Abstract

The time of firing of the output switch of a pulser is measured from some fiducial. The experiment is repeated and the difference in firing times is noted. The question under consideration in this paper is the accuracy of the measurement of this difference. The method of measuring the firing time in the presence of prepulse is by the zero crossing of a signal. It is desired to know the accuracy of the jitter measurement as a function of system bandwidth.

The conclusion is that for reasonable values of the parameters, the jitter error introduced by the bandwidth limitations is less than the oscilloscope reading error.

AFRLIDE 21384

SECTION I

INTRODUCTION

The problem discussed in this paper arose in connection with the measurement of the firing time of the final output switch on a Marx generator. When a Marx generator charges a peaking capacitor, there is a prepulse before the output switch fires. This arises from the capacitance of the output switch. The general character of the pulser waveform is the following: During the prepulse, the pulser waveform starts at zero with zero slope. The prepulse waveform then rises to a maximum. By Rolle's theorem, there is thus a zero in the second derivative of the pulser waveform between zero and the maximum. Near the maximum of the prepulse, the output switch is fired. As the main pulser waveform rises to its maximum, there are two inflection points: one is in the neighborhood of the output switch firing time and the other is in the neighborhood of the maximum. On the other side of the peak, there is also an inflection point.

The second derivative of the pulser waveform thus rises to a positive peak and then crosses the time axis. This point corresponds to the first inflection point of the prepulse waveform. The second derivative then crosses the time axis at a point corresponding to the firing of the output switch. It is this second crossing that is of concern in this paper. The second derivative rises to a maximum and then

crosses the axis at a point corresponding to the inflection point before the pulser waveform maximum. After an algebraic minimum which is negative, there is a zero crossing corresponding to the inflection point after the pulser waveform maximum.

In pulser applications, the variation of the second crossing from shot to shot can be considered as a measure of the output switch jitter. This paper will examine the consequences of finite bandwidth of the measuring system on the accuracy of this variation. This will be done with a one parameter representation of the filtering properties of the system. Two different representations of the pulser waveform will be studied: In the first case, the prepulse rises asymptotically to a maximum. In the second case, the prepulse has a maximum. In both representations, the pulser waveform and its first derivative are continuous.

To make the concept of jitter error quantitative, suppose that on a given shot the output switch fires at time t_0 but that the measured second derivative second zero crossing time is t_1 . Denote these quantities on a subsequent shot by $t_0 + \Delta t_0$ and $t_1 + \Delta t_1$. Since Δt_0 is the jitter, the accuracy of the jitter measurement depends on $\Delta t_1 - \Delta t_0$ rather than on $t_1 - t_0$. Thus the relative error in the jitter measurement is $(\Delta t_1 - \Delta t_0) / \Delta t_0 \equiv (\Delta t_1 / \Delta t_0) - 1$ which in the limit $\Delta t_0 \rightarrow 0$ is $(dt_1 / dt_0) - 1$. The emphasis of this paper will be on calculating $(dt_1 / dt_0) - 1$ from two analytic representations of the pulser waveform.

SECTION II

THEORY

Filtering

The first topic is a review of the concept of filtering. Let the input signal (the ideal pulser waveform second derivative) be denoted by $f(t)$ and the output signal (from the instrumentation) by $f^*(t)$. The general relationship between $f(t)$ and $f^*(t)$ may be expressed through $g(t)$ where $g(t) = f^*(t)$ for the special case that $f(t)$ is a unit impulse function. The simplest way to relate these functions is to first take a Laplace transform. The Laplace transform will be denoted by a tilde. Thus

$$\tilde{f}(s) = \int_0^{\infty} e^{-st} f(t) dt \quad (1)$$

The functions $\tilde{f}(s)$, $\tilde{g}(s)$ and $\tilde{f}^*(s)$ are related by

$$\tilde{f}^*(s) = \tilde{g}(s) \tilde{f}(s) \quad (2)$$

In the time domain

$$f^*(t) = \int_0^t g(t-t') f(t') dt' \quad (3)$$

The form that will be chosen for $\tilde{g}(s)$ is

$$\tilde{g}(s) = \Gamma / (\Gamma + s) \quad (4)$$

For $s = i\omega$, we have $|\tilde{g}(i\omega)| = \Gamma / (\Gamma^2 + \omega^2)^{\frac{1}{2}}$ which has the high frequency asymptote $|\tilde{g}(i\omega)| = \Gamma / \omega$ and the low frequency asymptote $|\tilde{g}(i\omega)| = 1$. These asymptotes intersect at $\omega = \Gamma$. We denote the frequency $f = \Gamma / 2\pi$ as the cutoff frequency.

In the time domain, Eq. (4) becomes

$$g(t) = \Gamma e^{-\Gamma t} \quad (5)$$

Note that $\int_0^{\infty} g(t) dt = 1$. Thus there are no low frequency errors.

Representations of Pulses

It is convenient to use dimensionless quantities. The normalization will be to t_r — a characteristic time for the rise of the main pulse. The dimensionless time T is defined by $T = t/t_r$. The pulser waveform in the first representation may be written

$$I_1(T) = QU(T) \left[1 - (1 + \alpha T)e^{-\alpha T} \right] + (1-Q)U(T-T_0) \left\{ 1 - \left[1 + (T-T_0) \right] e^{-(T-T_0)} \right\} \quad (6)$$

In Eq. (6), $U(T)$ is the step function. Thus $U(T) = 1$ for $T > 0$ and $U(T) = 0$ for $T < 0$. The parameter α is defined by $\alpha = t_r/t_{rp}$ where t_{rp} is a characteristic time for the rise of the prepulse. The parameter T_0 is defined by $T_0 = t_0/t_r$ where t_0 is the time at which the output switch fires. The parameter Q is related to the maximum of the prepulse. If the output switch never fired, the magnitude of the prepulse in the first representation would asymptotically approach Q .

Note that as $T \rightarrow \infty$, $I_1 \rightarrow 1$. Thus the curve of I_1 against T lacks one of the inflection points mentioned in the introduction. However, since the interest is in the neighborhood of T_0 , the lack of this inflection point does not affect the conclusions of this paper.

Just as it is convenient to use a dimensionless time, so it is also convenient to use a dimensionless Laplace transform variable. Consequently we define the dimensionless variable S by $S = st_r$. In terms of this variable, the Laplace transform of Eq. (6) is given by

$$\tilde{I}_1(s)/t_r = \frac{Q\alpha^2}{S(S+\alpha)^2} + \frac{(1-Q)e^{-ST_0}}{S(S+1)^2} \quad (7)$$

The second representation of the pulser waveform used in this paper is given by

$$I_2(T) = (Q/Q_0)U(T) \left\{ e^{-\delta t} - [1+(\alpha-\delta)T] e^{-\alpha t} \right\} + U(T-T_0) \left\{ 1 - [1+(T-T_0)] e^{-(T-T_0)} \right\} \quad (8)$$

The parameter δ is defined by $\delta = t_r/t_d$ where t_d is the decay time of the prepulse. The quantity Q_0 is the maximum of $e^{-\delta T} - [1+(\alpha-\delta)T] e^{-\alpha T}$.

Note that $I_2 \rightarrow 1$ as $T \rightarrow \infty$.

The Laplace transform of Eq. (8) is given by

$$\tilde{I}_2(s)/t_r = \frac{(Q/Q_0)(\alpha-\delta)^2}{(S+\delta)(S+\alpha)^2} + \frac{e^{-ST_0}}{S(S+1)^2} \quad (9)$$

Filtered Pulses

As explained in the introduction, the signal used in the jitter determination is not the pulser waveform but its second derivative.

From Eq. (6) and Eq. (8) we have

$$d^2 I_1 / dT^2 = QU(T) \alpha^2 (1 - \alpha T) e^{-\alpha T} + (1-Q)U(T-T_0) \left[1 - (T-T_0) \right] e^{-(T-T_0)} \quad (10)$$

$$d^2 I_2 / dT^2 = (Q/Q_0)U(T) \left\{ \delta^2 e^{-\delta T} + \left[\alpha^2 - 2\alpha\delta - \alpha^2(\alpha-\delta)T \right] e^{-\alpha T} \right\} + U(T-T_0) \left[1 - (T-T_0) \right] e^{-(T-T_0)} \quad (11)$$

Introducing the dimensionless parameter $\gamma = \Gamma t_r$, from Eqs. (3), (5), (10),

(11) we have for the filtered signals

$$(d^2 I_1 / dT^2)^* = QU(T) \left[\frac{\alpha^2 \gamma^2}{(\gamma - \alpha)^2} (e^{-\alpha T} - e^{-\gamma T}) - \frac{\alpha^3 \gamma T}{\gamma - \alpha} e^{-\alpha T} \right] + (1-Q)U(T-T_0) \left\{ \frac{\gamma^2}{(\gamma - 1)^2} \left[e^{-(T-T_0)} - e^{-\gamma(T-T_0)} \right] - \frac{\gamma(T-T_0)}{\gamma - 1} e^{-(T-T_0)} \right\} \quad (12)$$

$$(d^2 I_2 / dT^2)^* = (Q/Q_0)U(T) \left[\frac{\gamma \delta^2}{\gamma - \delta} (e^{-\delta T} - e^{-\gamma T}) + \frac{(\alpha^2 \gamma^2 - 2\alpha\delta\gamma + \alpha^2 \delta\gamma)}{(\gamma - \alpha)^2} (e^{-\alpha T} - e^{-\gamma T}) - \frac{\alpha^2 \gamma (\alpha - \delta) T e^{-\alpha T}}{\gamma - \alpha} \right] + U(T-T_0) \left\{ \frac{\gamma^2}{(\gamma - 1)^2} \left[e^{-(T-T_0)} - e^{-\gamma(T-T_0)} \right] - \frac{\gamma(T-T_0)}{\gamma - 1} e^{-(T-T_0)} \right\}$$

(13)

The analysis of jitter measurement accuracy will be based on the second zero crossings of $(d^2I_1/dT^2)^*$ and $(d^2I_2/dT^2)^*$ as given by Eq. (12) and Eq. (13).

Qualitative Error Discussion

Let us first consider the unfiltered pulse as given by Eq. (10).

In Eq. (10), take the case that $T_0 > 1/\alpha$. The first zero crossing for the unfiltered pulse can be seen from Eq. (10) to be at $T = 1/\alpha$. To see how this is affected by filtering, take the special case that $\gamma = \alpha$ in Eq. (12).

By L'Hospital's rule, Eq. (12) becomes

$$\begin{aligned}
 (d^2I_1/dT^2)^* &= \frac{1}{2} QU(T) \alpha^2 (2\alpha T - \alpha^2 T^2) e^{-\alpha T} \\
 &+ (1-Q)U(T-T_0) \left\{ \frac{\gamma^2}{(\gamma-1)^2} \left[e^{-(T-T_0)} - e^{-\gamma(T-T_0)} \right] \right. \\
 &\left. - \frac{\gamma(T-T_0)}{\gamma-1} e^{-(T-T_0)} \right\} \tag{14}
 \end{aligned}$$

From Eq. (14) it is seen that in the special case $\gamma = \alpha$, the filtered pulse has the first zero crossing at $T = 2/\alpha$ provided that $T_0 > 2/\alpha$. On the other hand, if $1/\alpha < T_0 < 2/\alpha$, the unfiltered pulse has a first zero crossing at $T = 1/\alpha$ and a second zero crossing at $T = T_0$ but the filtered pulse for the case $\gamma = \alpha$ does not have these corresponding crossings.

This special case illustrates the point that for a given separation of the first and second zero crossings of the unfiltered pulse, too small a bandwidth can wash these crossings away. To put it another way, the greater

the separation of the first and second zero crossings in the unfiltered pulse, the less bandwidth is required for a given jitter measurement accuracy.

In the numerical studies based on Eqs. (11) and (12), it was found that $(dt_1/dt_0)-1$ could have both positive and negative values. Since it may not be clear why this is so, let us introduce an approximation to $(d^2I/dT^2)^*$ to gain insight into how $(dt_1/dt_0)-1$ varies with a change of parameters. The function I may be either I_1 or I_2 . We first introduce the quantities p_1 and p_2 which are the slopes of $(d^2I/dT^2)^*$ at $T = T_1-0$ and $T = T_0+0$ respectively. For the representations used in this paper, p_1 and p_2 are distinct. We define the parameter Z by

$$Z = (d^2I/dT^2)^* \Big|_{T = T_0} \quad (14.1)$$

Since Z is the value of the prepulse at $T = T_0$, then

$$dZ/dT_0 = p_1 \quad (14.2)$$

For $T > T_0$ we may approximate $(d^2I/dT^2)^*$ by

$$(d^2I/dT^2)^* = Z + p_2(T-T_0) \quad (14.3)$$

Since at $T = T_1$, $(d^2I/dT^2)^* = 0$, Eq. (14.3) implies that

$$T_1 - T_0 = Z/p_2 \quad (14.4)$$

Equation (14.4) is exact in the limit that $Z \rightarrow 0$. If we differentiate

Eq. (14.4) with respect to T_0 we have

$$(dT_1/dT_0) - 1 = -(dZ/dT_0)/p_1 + Z(dp_1/dT_0)/p_1^2 \quad (14.5)$$

Since $(dT_1/dT_0) = (dt_1/dt_0)$, the combination of Eqs. (14.2) and (14.5) gives

$$\lim_{Z \rightarrow 0} \left[(dt_1/dt_0) - 1 \right] = -p_1/p_2 \quad (15)$$

To apply Equation (15), let us fix all parameters except T_0 . Let T_0 approach the first zero crossing which implies that Z goes to zero. In the neighborhood of the first zero crossing, p_1 is negative and p_2 is positive. From Eq. (15) this means if T_0 is in the neighborhood of the first zero crossing then $(dt_1/dt_0) - 1$ is positive. On the other hand, if T_0 is in the neighborhood of infinity, Z is in the neighborhood of zero but p_1 and p_2 are both positive so that $(dt_1/dt_0) - 1$ is negative.

We have just seen that it is possible to choose the parameters so that $(dt_1/dt_0) - 1$ is negative. Let us choose a set of parameters so that this is so and fix all the parameters except the bandwidth parameter γ . Let us now decrease γ . As seen from the example for which $\gamma = \alpha$, as the bandwidth parameter decreases, the time at which the first zero crossing occurs increases. As the time of the first zero crossing approaches T_0 , we would expect that the sign of $(dt_1/dt_0) - 1$ would change from negative to positive. Thus there would be a change in the sign of $(dt_1/dt_0) - 1$ with the variation of the bandwidth parameter. This behavior was observed in the numerical studies.

Asymptotic Forms for Large Bandwidth

Let us now examine the question of how the jitter measurement accuracy varies for large bandwidth, which corresponds to large values of the parameter γ . We expand T_1 in a series in $1/\gamma$ and write

$$T_1 = T_0 + T_{11}/\gamma + \dots \quad (16)$$

Equation (16) is substituted into Eq. (12) and Eq. (13) and these equations are expanded in power series in $1/\gamma$. Since this expansion is valid only for large γ , we neglect the terms $e^{-\gamma T_0}$. From Eq. (12) this procedure gives

$$T_{11} = \ln(1-Q) - \ln \left[\alpha^2 Q e^{-\alpha T_0} (1 - \alpha T_0) + 1 - Q \right] \quad (17)$$

Since $dt_1/dt_0 = dT_1/dT_0$ then Eq. (17) gives

$$dt_1/dt_0 - 1 = \frac{1}{\gamma} dT_{11}/dT_0 = \frac{1}{\gamma} \left[\frac{\alpha^3 Q e^{-\alpha T_0} (2 - \alpha T_0)}{\alpha^2 Q e^{-\alpha T_0} (1 - \alpha T_0) + 1 - Q} \right] \quad (18)$$

The corresponding equations for Eq. (13) are

$$T_{11} = -\ln \left\{ 1 + (Q/Q_0) \left[\delta^2 e^{-\delta T_0} + (\alpha^2 - 2\alpha\delta - \alpha^2 T_0 (\alpha - \delta)) e^{-\alpha T_0} \right] \right\} \quad (19)$$

$$dt_1/dt_0 - 1 = \frac{(Q/Q_0)}{\gamma} \left\{ \frac{\delta^3 e^{-\delta T_0} + [2\alpha^3 - 3\alpha^2\delta - \alpha^3 T_0 (\alpha - \delta)] e^{-\alpha T_0}}{1 + (Q/Q_0) [\delta^2 e^{-\delta T_0} + (\alpha^2 - 2\alpha\delta - \alpha^2 (\alpha - \delta) T_0) e^{-\alpha T_0}]} \right\} \quad (20)$$

Let us draw some conclusions from and make some simplifications of Eqs. (18) and (20). First note that in both Eqs. (18) and (20) that as $T_0 \rightarrow \infty$,

$dt_1/dt_0 - 1 \rightarrow 0$. Note also the change of sign of $(dt_1/dt_0) - 1$ as T_0 increases. In particular note in Eq. (18) that for large γ , there is a change of sign in the neighborhood of $\alpha T_0 = 2$.

As has been discussed previously, if we fix the other parameters, we would expect the jitter error to increase as T_0 approaches the first zero crossing. In Eq. (18) let us take $\alpha T_0 = 1$. This gives

$$(dt_1/dt_0) - 1 = \frac{\alpha^3 Q e^{-1}}{\gamma(1-Q)} \quad (21)$$

In the region where the asymptotic expansion is valid, it is expected that Eq. (21) would give an upper limit to $(dt_1/dt_0) - 1$.

A similar approach may be taken to Eq. (20). From Eq. (11) it is seen that as $\gamma \rightarrow \infty$, T_0 will be in the neighborhood of the first zero crossing provided that

$$\delta^2 e^{-\delta T_0} + \left[\alpha^2 - 2\alpha\delta - \alpha^2(\alpha - \delta)T_0 \right] e^{-\alpha T_0} = 0 \quad (22)$$

Combining Eqs. (20) and (22) gives

$$(dt_1/dt_0) - 1 = \frac{(Q/Q_0)}{\gamma} \left[(\delta^3 - \alpha\delta^2)e^{-\delta T_0} + (\alpha^3 - \alpha^2\delta)e^{-\alpha T_0} \right] \quad (23)$$

Effect of Prepulse on Frequency Domain

If we look at Eq. (7) we see that the prepulse changes the frequency domain characteristics of the pulser waveform. As a basis for comparison, let us define $\tilde{I}_0(s)$ by

$$\tilde{I}_0(s)/t_r = \frac{1}{S(S+1)^2} \quad (24)$$

By comparing with Eqs. (7) and (9) it is seen that Eq. (24) may be regarded as a frequency domain waveform with no prepulse. To see the effect of the prepulse, let us divide Eq. (7) by Eq. (24) and note that $st_0 = ST_0$. Thus as s becomes infinite we may write

$$\tilde{I}_1(s)/\tilde{I}_0(s) = Q\alpha^2 + (1-Q)e^{-st_0} \quad (25)$$

For the case $s = i\omega$, the minimum absolute value is given by

$$|\tilde{I}_1/\tilde{I}_0| = |1 - Q(1 + \alpha^2)| \quad (26)$$

NUMERICAL RESULTS

As stated earlier, the approach to the problem is to set the right hand sides of Eqs. (12) and (13) equal to zero and solve for T in the neighborhood of T_0 . Newton's method was used to solve the equations. The initial value used was $T = T_0 + 0$. The convergence criterion used was that the change in T between successive Newtonian iterations be less than 10^{-4} . The calculation was repeated with T_0 increased by ΔT_0 . Denoting the corresponding value of T_1 by $T_1 + \Delta T_1$ then $(\Delta T_1 / \Delta T_0) - 1$ is an estimate of $(dt_1/dt_0) - 1$. By choosing various values of ΔT_0 it was found that the choice of $\Delta T_0 = 10^{-2}$ gives a value of $(\Delta T_1 / \Delta T_0) - 1$ which differs from $(dt_1/dt_0) - 1$ by less than 1%.

The numerical work was carried out on the AFWL CDC 6600.

Discussion of Graphs

The curves presented here are only a sample of the calculations performed. The reason for only giving a sample will be discussed in the section on conclusions.

Figure 1 is a schematic of a scope trace. The point marked t_1 is the second zero crossing. For the other curves, some things must be said on how to calculate the parameters. A common way of specifying the rise is with the 10-90% rise time. For the representation used, the relationship in the absence of prepulse is given by

$$t(10-90) = 3.3579 t_r \quad (27)$$

In Eq. (27) $t(10-90)$ is the 10-90% rise time.

The parameter Γ is related to the cutoff frequency f by the relationship

$$\Gamma = 2\pi f \quad (28)$$

Thus the parameter γ is given by

$$\gamma = \Gamma t_r = \frac{2\pi f t(10-90)}{3.3579} = 1.871 f t(10-90) \quad (29)$$

For example if $t(10-90) = 10$ nanoseconds $= 10^{-8}$ seconds and $f = 10$ megaHertz $= 10^7$ Hertz then $\gamma = 0.1871$. If we look on Figure 2 we see that for $\gamma = 0.1871$ and $\alpha = 0.3$ that $(dt_1/dt_0)^{-1} = 1.3510^{-3}$, using the first representation for the prepulse.

As explained previously, the value $\alpha = 0.3$ means that the main pulse rise time is 30% of the prepulse rise time. Figure 2 is for $Q = 0.2$ and $\alpha t_0 = 3$. Thus in this case the prepulse maximum is 0.2 of the final pulser waveform maximum. The value $\alpha T_0 = 3$ corresponds to firing the main switch when the prepulse has reached about 80% of its maximum.

In the calculations used to plot Figures 2 and 3, the parameter γ varied in steps of 0.1 in the range $0.1 \leq \gamma \leq 1.0$. In the range $1.0 \leq \gamma \leq 10.0$, the step was 1.0. The step was 0.05 for Figure 2 in the range $1 < \gamma < 2$ and for Figure 3 in the range $2 < \gamma < 3$. Both Figures 2 and 3 show a cutoff in the curves on the left. For example, in Figure 2 the curve $\alpha = 0.4$ does not extend to the next step of $\gamma = 0.1$. The reason is that for $\alpha = 0.4$ the bandwidth of $\gamma = 0.1$ is so small that the first and second zero crossings are washed out. As indicated in Figures 2 and 3, the curves on the right correspond to negative values of $(dt_1/dt_0) - 1$ while those on the left correspond to positive values of $(dt_1/dt_0) - 1$.

In figures 3, 5, and 7, the symbol " T_{\max} " occurs. The number T_{\max} is the value of T for which $e^{-\delta T} - [1 + (\alpha - \delta)T] e^{-\alpha T}$ is a maximum. Thus T_{\max} is the dimensionless time when the maximum of the double exponential prepulse occurs.

Using Eqs. (18) and (20) the asymptotic forms were calculated. Figure 4 is the asymptotic form corresponding to Figure 2 while Figure 5 corresponds to Figure 3. The comparison of the curves shows that there is good agreement between the asymptotic forms and the exact forms for

$\gamma = 10$ but that for lower values of γ the asymptotic form overestimates $|(dt_1/dt_0)-1|$. The results of calculations for the parameter values not shown indicate that this is generally true.

In Figures 6 and 7 are shown the difference between the main switch firing time and the second zero crossing. Figure 6 corresponds to Figure 2 while Figure 7 corresponds to Figure 3. As expected, the curves go to zero as γ becomes infinite. What may be surprising is that the curves have a maximum. A way of explaining it is from the relationship $t_f < t_0 < t_1$ where t_f is the first zero crossing. As γ decreases, $t_1 - t_f \rightarrow 0$. If we define γ_c as the value of γ for which $t_f = t_0 = t_1$, then for $\gamma < \gamma_c$, the first and second zero crossings are washed out.

The final figure is a graph of Q_0 against δ/α . The quantity Q_0 is the maximum of $e^{-\delta T} - [1+(\alpha-\delta)T] e^{-\alpha T}$. We may write $\delta/\alpha = t_{rp}/t_d$ where t_{rp} is a characteristic time of the rise of the prepulse and t_d is the decay time of the prepulse.

Oscilloscope Reading Error

If Δt_1 and Δt_0 are small we may write

$$\Delta t_1 = (dt_1/dt_0) \Delta t_0 \equiv \Delta t_0 + [(dt_1/dt_0)-1] \Delta t_0 \quad (30)$$

Up to now, the error analysis has been based on Eq. (30). Nothing has been said about the error introduced by reading the oscilloscope. Let us denote the actual observed jitter as Δt_2 . For the case of no reading

error $\Delta t_2 = \Delta t_1$. We start with the identity

$$\Delta t_2 \equiv (\Delta t_2 - \Delta t_1) + \Delta t_1 \quad (31)$$

Combining Eqs. (30) and (31) gives

$$\Delta t_2 = (\Delta t_2 - \Delta t_1) + \left[(dt_1/dt_0) - 1 \right] \Delta t_0 + \Delta t_0 \quad (32)$$

The term $\Delta t_2 - \Delta t_1$ is the oscilloscope reading error while the term $\left[(dt_1/dt_0) - 1 \right] \Delta t_0$ is the error introduced by the second zero crossing method. It is to be expected that $\Delta t_2 - \Delta t_1$ is a few percent of Δt_0 .

SECTION III

CONCLUSIONS

The regions where it is to be expected that the error of the second zero crossing method would be a few percent greater than of Δt_0 are where the rise time of the prepulse is comparable to the rise time of the main pulse or where the main switch fires well before the prepulse maximum or both. We may want to fire at the prepulse maximum since this approximately corresponds to the maximum current from the Marx into the peaking capacitor. If the rise of the main pulse is not significantly faster than the prepulse this means that the Marx charges the peaking capacitor about as fast as the peaking capacitor discharges into the load.

To put it another way, if for some pulse a problem arises from the second zero crossing method then perhaps the pulse itself is bad.

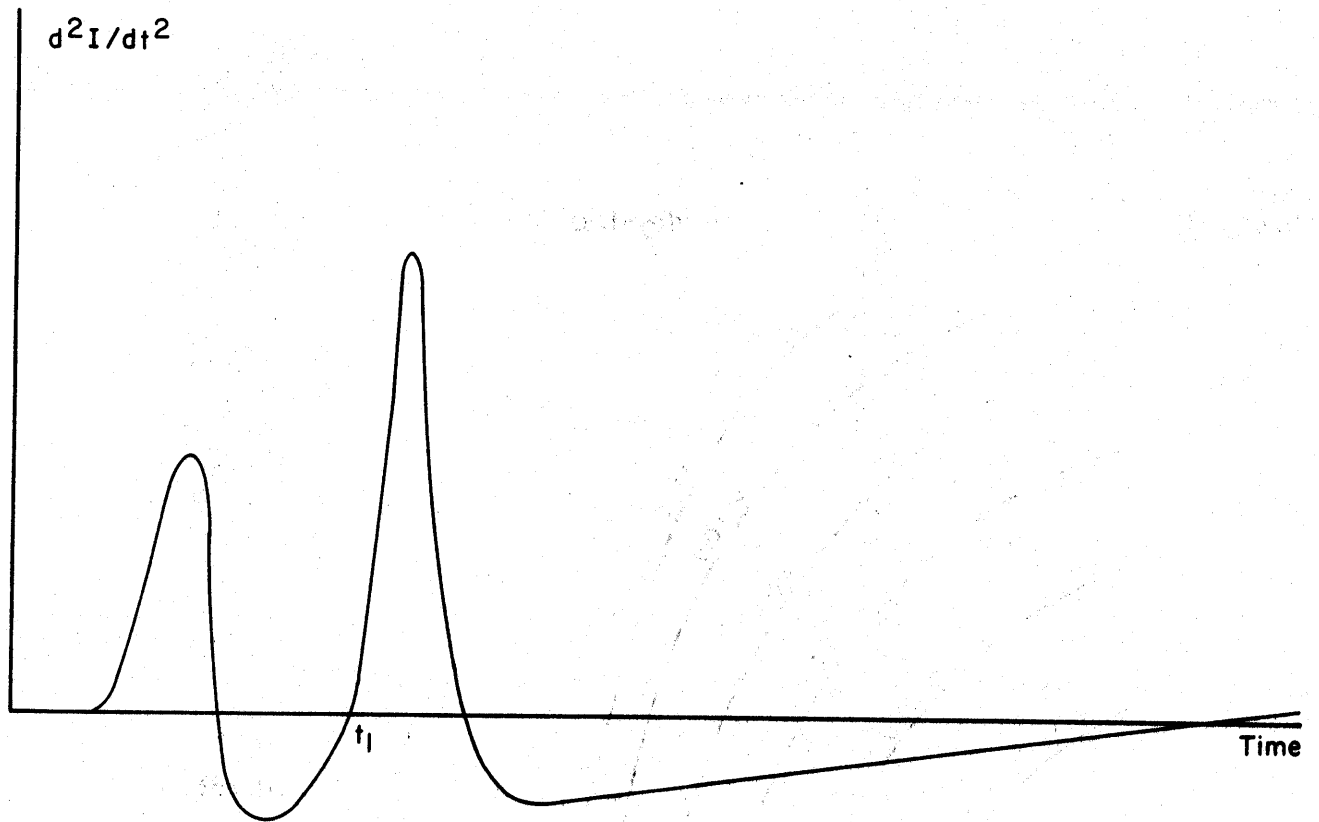


Figure 1. Qualitative graph of pulser waveform second derivative against time.

$\alpha T_0 = 3.0$
 $Q = 0.2$

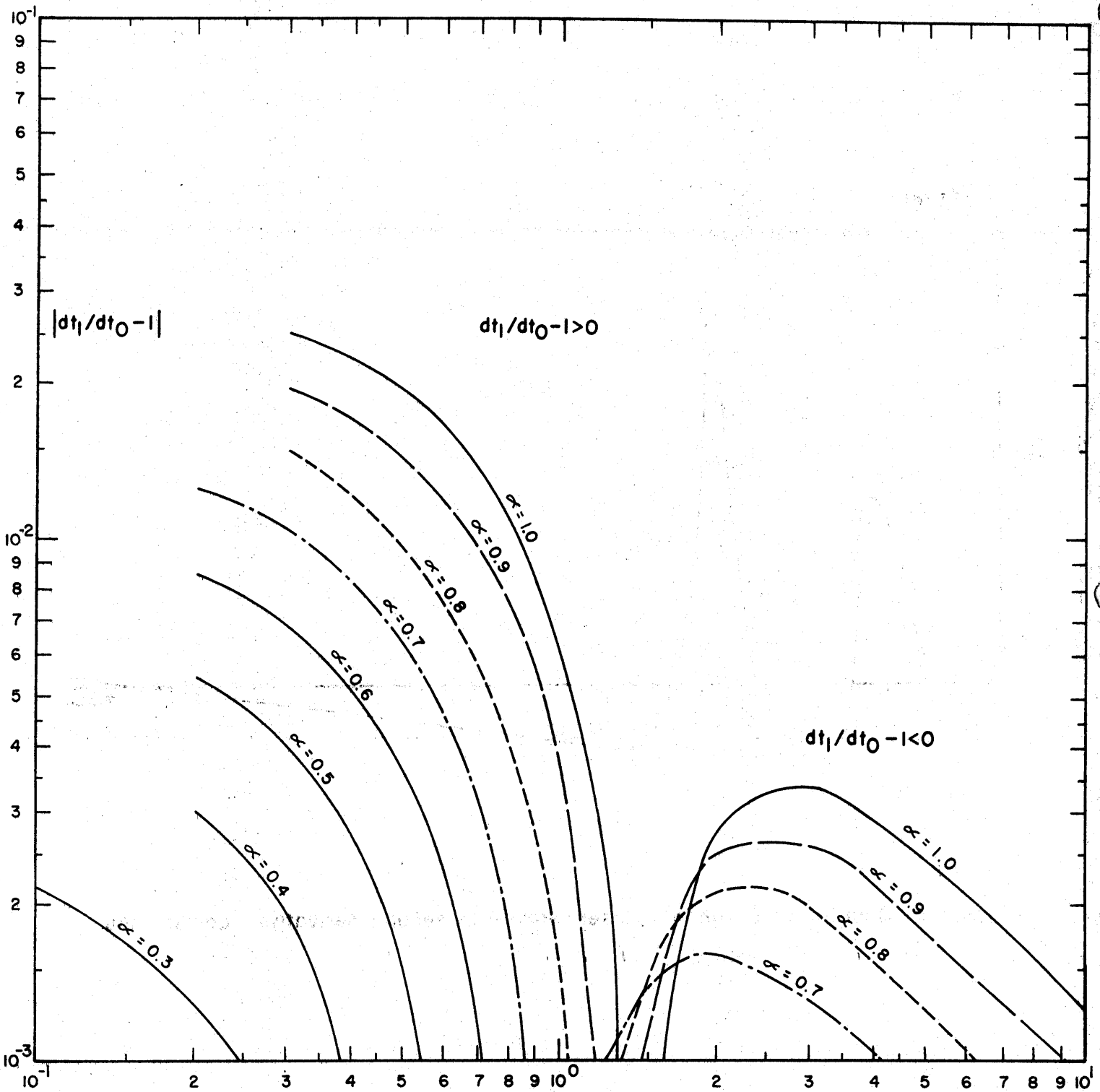


Figure 2. Jitter error against bandwidth for simple prepulse. (I_1 Waveform)

$$T_0 = (3/4) T_{max}$$

$$Q = 0.2$$

$$\delta = 0.2$$

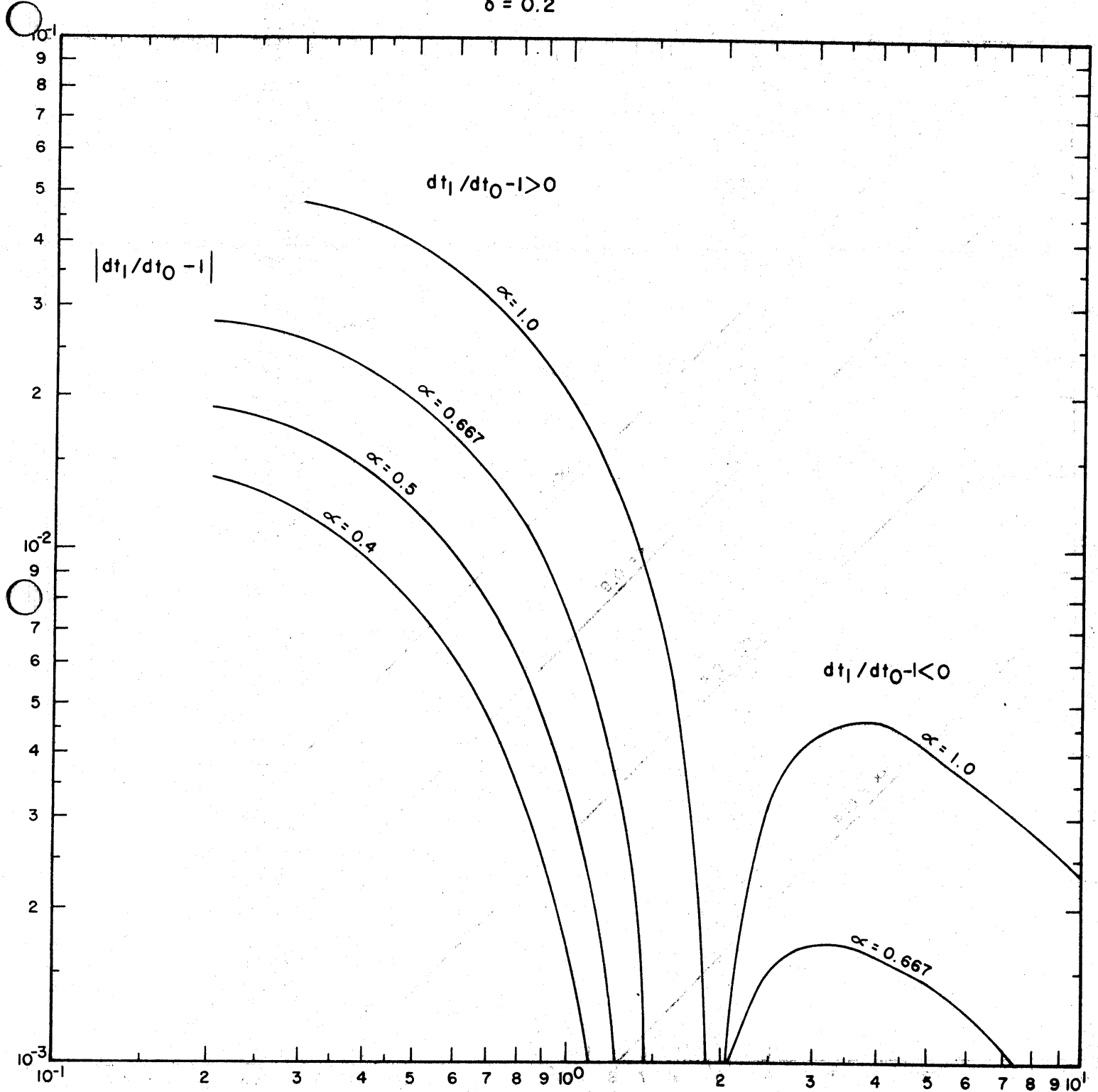


Figure 3. Jitter error against bandwidth for double exponential prepulse. (I_2 Waveform)

$\alpha T_0 = 3.0$
 $Q = 0.2$

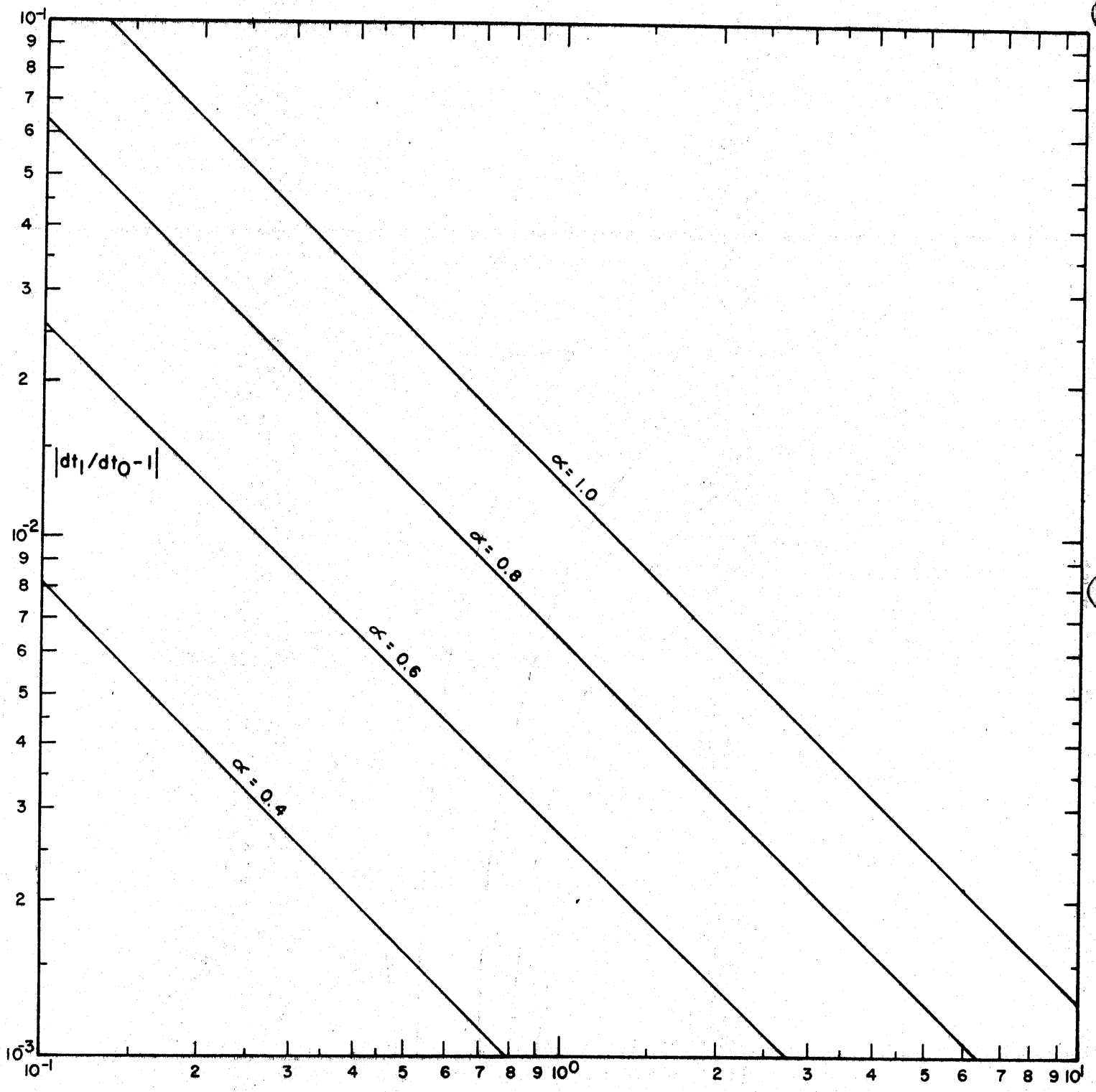


Figure 4. Asymptotic jitter error against bandwidth for simple prepulse. (I_1 Waveform)

$T_0 = (3/4) T_{max}$
 $Q = 0.2$
 $\delta = 0.2$

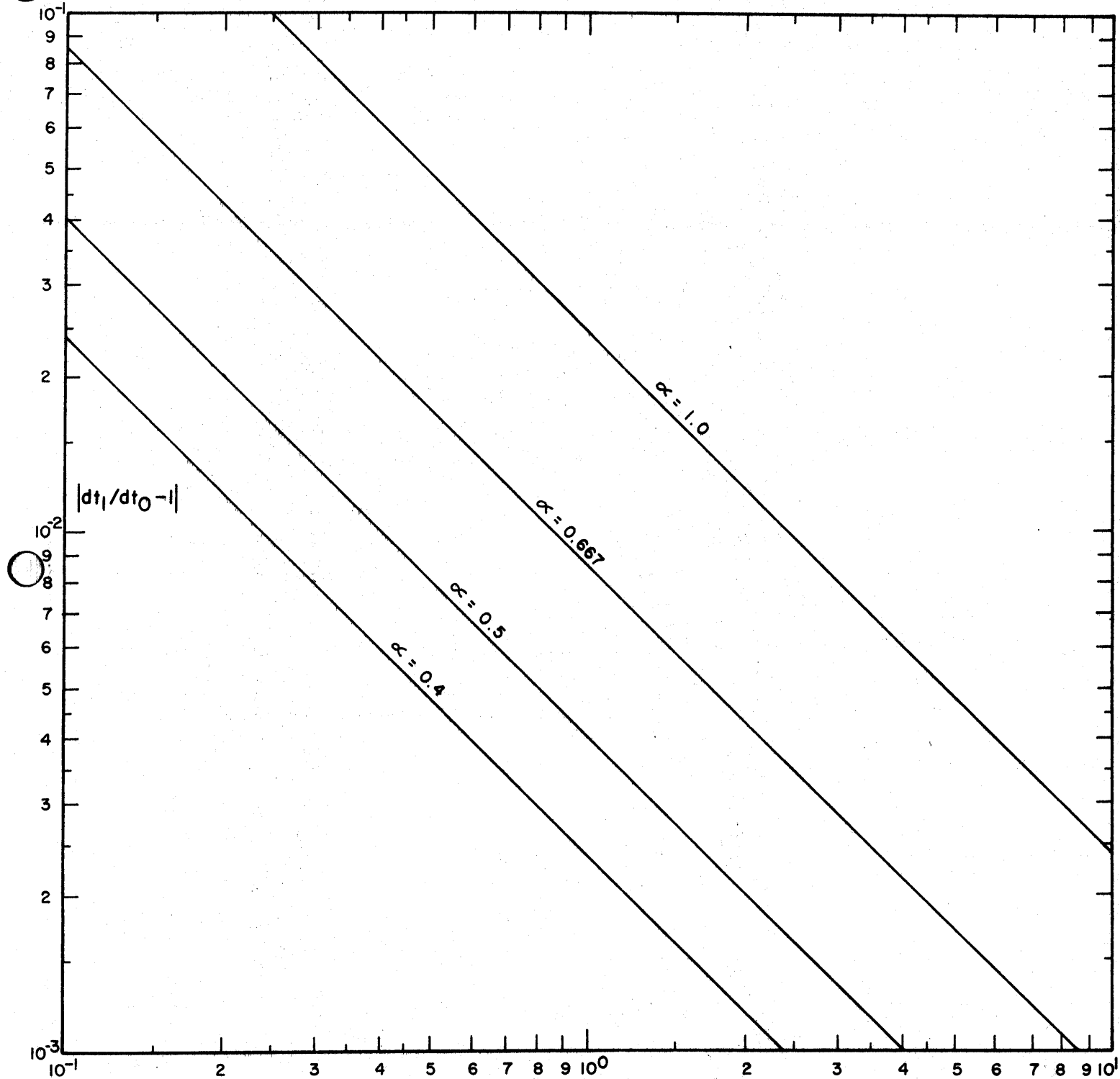


Figure 5. Asymptotic jitter error against bandwidth for double exponential prepulse. (I_2 Waveform)

$\alpha T_0 = 3.0$
 $Q = 0.2$

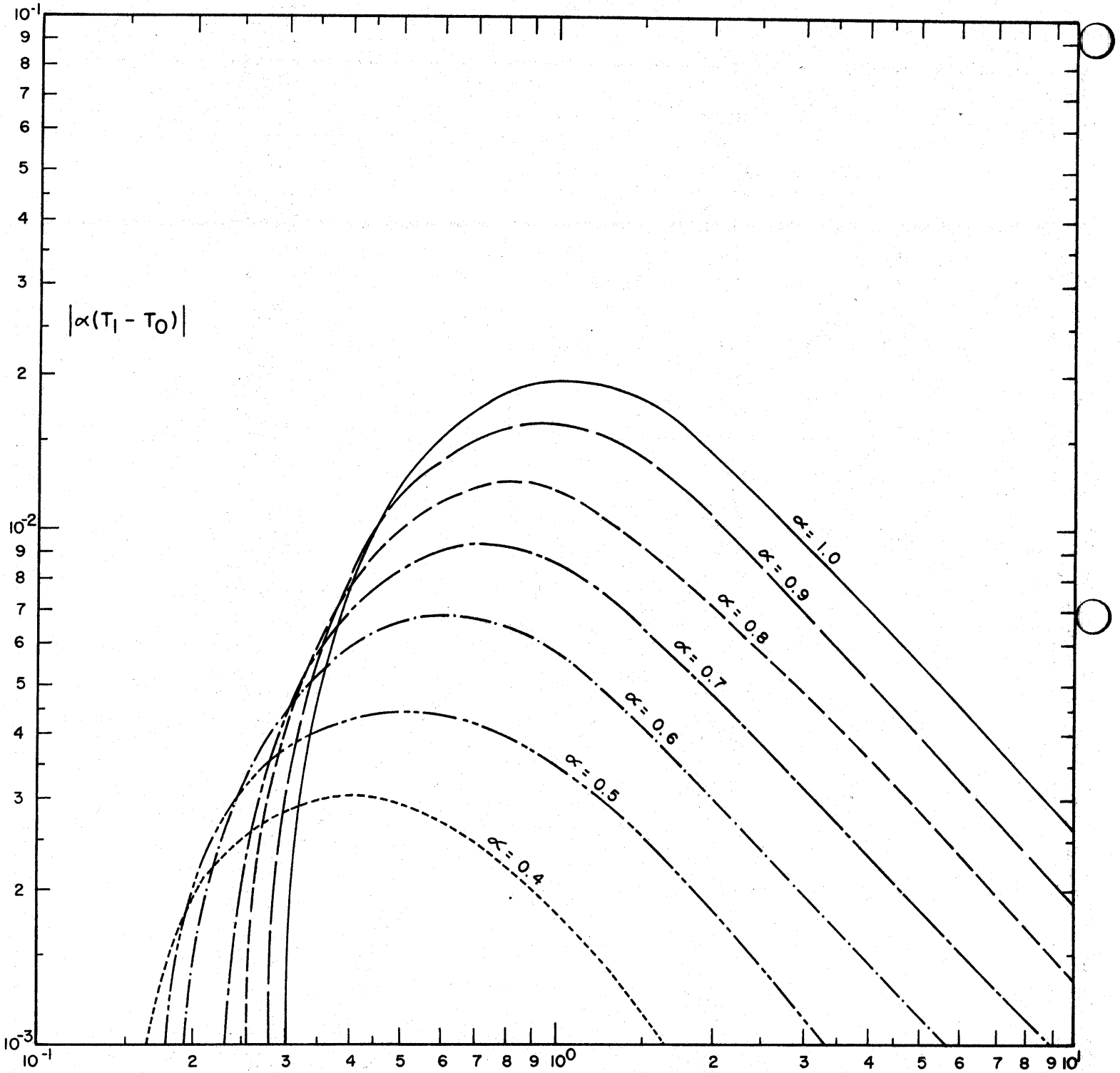


Figure 6. Difference between output switch firing time and measured firing time against bandwidth for simple prepulse. (I_1 Waveform)

$$T_0 = (3/4) T_{max}$$

$$Q = 0.2$$

$$\delta = 0.2$$

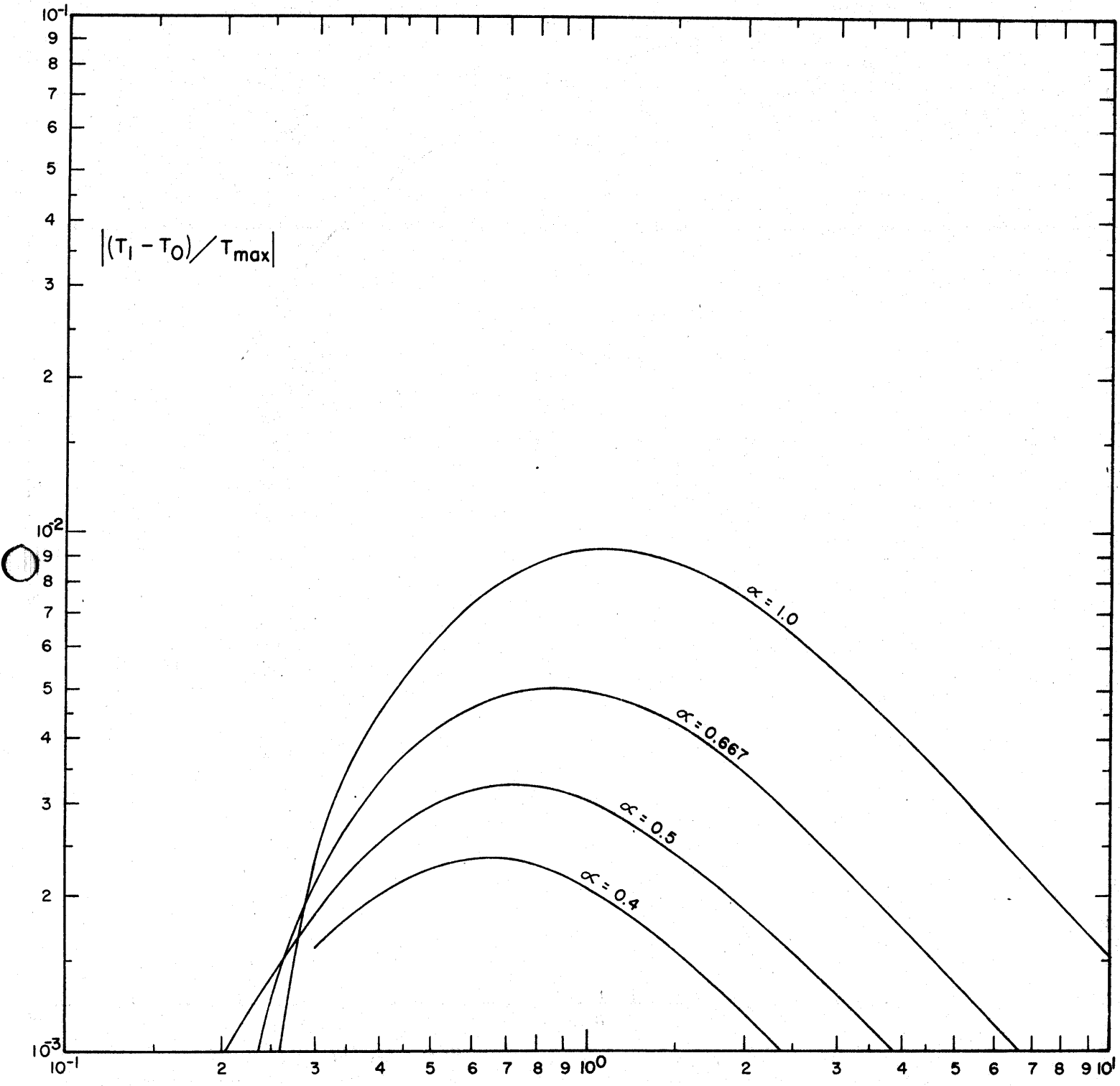


Figure 7. Difference between output switch firing time and measured firing time against bandwidth for simple prepulse. (I_2 Waveform)

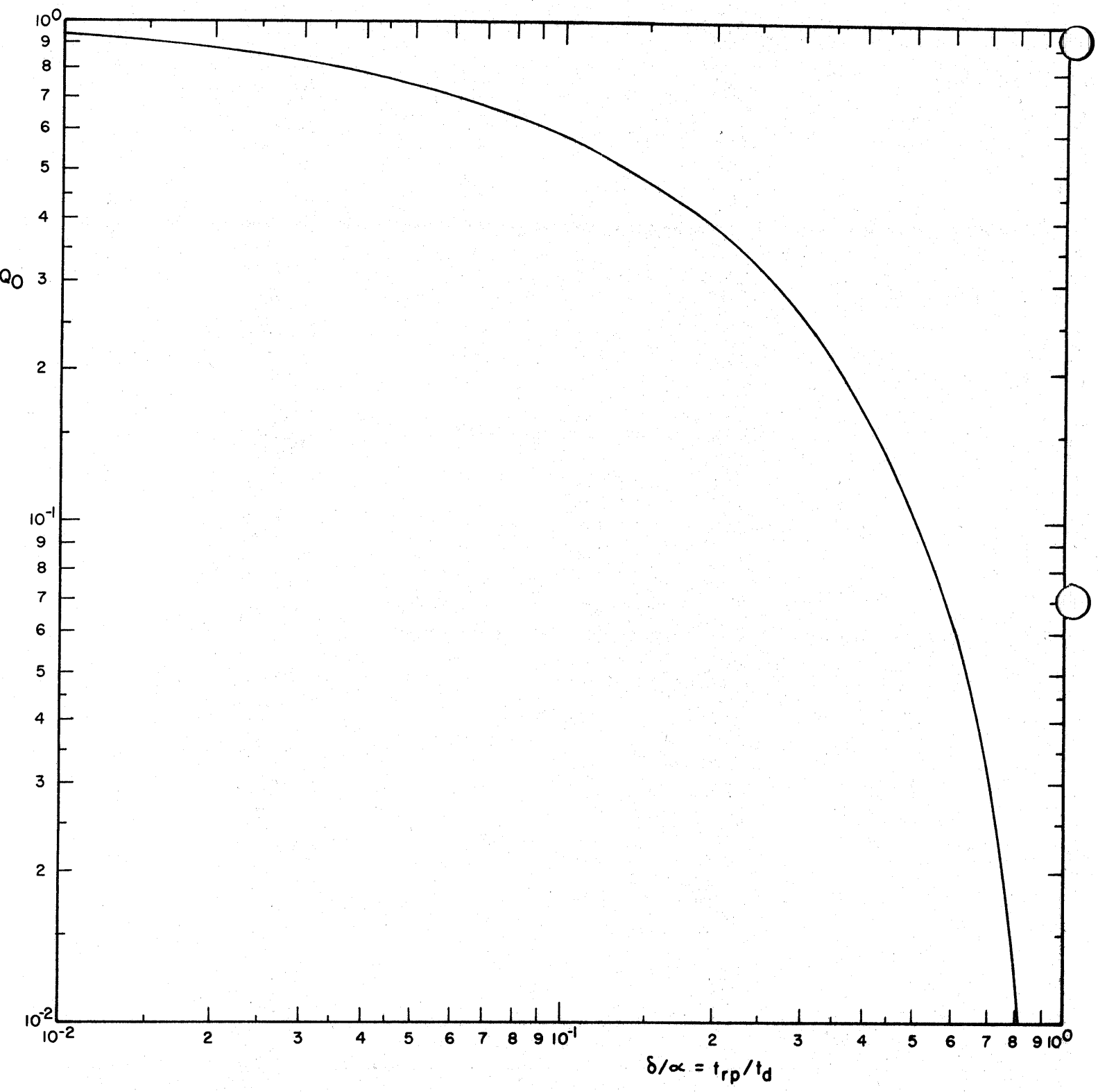


Figure 8. Maximum of double exponential prepulse against ratio of prepulse decay to prepulse rise. (I_2 Waveform)